J Biol Phys (2018) 44:433–448
https://doi.org/10.1007/s10867-018-9500-0

ORIGINAL PAPER

Changes of cationic transport in *AtCAX5* transformant yeast by electromagnetic field environments

Munmyong Choe[1] · **Won Choe**[1] · **Songchol Cha**[1] · **Imshik Lee**[2]

Received: 19 January 2018 / Accepted: 4 May 2018 / Published online: 7 June 2018

Abstract The electromagnetic field (EMF) is newly considered as an exogenous environmental stimulus that is closely related to ion transportation on the cellular membrane, maintaining the internal ionic homeostasis. Cation transports of Ca^{2+} and other metal ions, Cd^{2+}, Zn^{2+}, and Mn^{2+}were studied in terms of the external Ca^{2+} stress, $[Ca^{2+}]_{ext}$, and exposure to the physical EMF. A specific yeast strain K667 was used for controlling *CAX5* (cation/H^+ exchanger) expression. Culture samples were exposed to 60 Hz, 0.1 mT sinusoidal or square magnetics waves, and intracellular cations of each sample were measured and analyzed. *AtCAX5* transformant yeast grew normally under the metallic stress. However, the growth of the control group was significantly inhibited under the same cation concentration; 60 Hz and 0.1 mT magnetic field enhanced intracellular cation concentrations significantly as exposure time increased both in the *AtCAX5* transformed yeast and in the control group. However, the *AtCAX5*-transformed yeast showed higher concentration of the intracellular cations than the control group under the same exposure EMF. *AtCAX5*-transformed yeasts displayed an increment in $[Ca^{2+}]_{int}$, $[K^+]_{int}$, $[Na^+]_{int}$, and $[Zn^{2+}]_{int}$ concentration under the presence of both sinusoidal and square-waved EMF stresses compared to the control group, which shows that AtCAX5 expressed in the vacuole play an important role in maintaining the homeostasis of intracellular cations. These findings could be utilized in the cultivation of the crops which were resistant to excessive exogenous ions or in the production of biomass containing a large proportion of ions for nutritional food or in the bioremediation process in metal-polluted environments.

Keywords Cation transportation · Extremely low frequency electromagnetic field (ELF-EMF) · *Saccharomyces cerevisiae* K667 · *AtCAX*5 transformant yeast

✉ Imshik Lee
ilee@nankai.edu.cn

[1] R & D Center, Pyongyang University of Science & Technology, Pyongyang, Democratic People's Republic of Korea

[2] Institute of Physics, Nankai University, Weijin Rd., Tianjin 300071, China

1 Introduction

Ion transport is essential for ion metabolism for the survival of cells, and extracellular stresses, mediating the ion flux in and out of the cell, have received attention from many researchers. With technological progress, the chances of biological systems being exposed to physical stimuli such as man-made electromagnetic field (EMF) are increasing; thus an investigation into the influence of such physical stimulus on biological systems has been reported [1–3]. In particular, several studies have discussed how extremely low frequency electromagnetic fields (ELF-EMFs) can affect the various biological functions of cells, such as cell proliferation, gene transcription, enzyme activity, and ion transport [1, 4, 5]. EMF effects on ion homeostasis may be allied to the mechanisms underlying the physical stress-induced biological effects [6].

Ion transport is closely related to cellular signaling, and many different ion channels are involved in this process [5, 7]. It has already been reported that intracellular Ca^{2+} ($[Ca^{2+}]_{int}$) levels in rat thymic lymphocytes, human T-lymphocytes, Jurkat cells, and rat pituitary cells were modified by EMF exposure. There are some attempts to illustrate the action of EMFs on intracellular ion concentration change with the correlation of their effect on ion transporters [2, 8–10]. Grassi et al. studied the relation between the effect of 60-Hz EMF on neuronal and neuroendocrine cell turnover, and voltage-gated Ca^{2+} channels [10, 11]. Although many ion channels have been studied, there are still other different types of ion transporters including ion exchangers and ion pumps that need to be investigated with relation to EMF effects. Among those ion transporters, vacuolar cation exchangers are known to regulate the intracellular ion homeostasis that can sequester the excess of exogenic cations into vacuoles so as to confer the tolerance to a range of ion stresses [12, 13]. In spite of their important role in ion homeostasis in cells, the correlation between cation exchangers with electromagnetic fields is still uncertain when compared to the information about the electromagnetic field effects on other ion channels such as Na^+/K^+ pumps and voltage-gated channels.

CAX5 is a member of the vacuolar cation exchangers (*CAX*) group expressed in plants and fungi rather than in animal cells, which belongs to the Ca^{2+}/cation antiporter (*CaCA*) superfamily. In plants and fungi, vacuolar cation exchangers play an important role in maintaining the proper cytosolic ion concentrations by the compartmentation of potentially toxic cations into various cellular organelles such as vacuoles, endoplasmic reticulum, and mitochondria. Therefore, *CAX* plays an important role in cationic homeostasis in plants and fungi, but not in animal cells. In the *Arabidopsis thaliana* genome, there are six *CAX* open reading frames, and the transporter proteins are predominantly localized on the vacuoles. Those six CAX genes, named *AtCAX1* (At2g38170), *AtCAX2* (At3g13320), *AtCAX3* (At3g51860), *AtCAX4* (At5g01490), *AtCAX5* (At1g55730), and *AtCAX6* (At1g55720) encode the cation transporters, which have the protein lengths of 463, 441, 459, 446, 441, and 448, respectively (http://www.uniprot.org/uniprot). Using yeast mutants deleted for the vacuolar Ca^{2+} ATPase (PMC1) and H^+/Ca^{2+}antiporter (*VCX1*), Ca^{2+} transport ability into vacuoles of various *CAX*s were reviewed [14]. *CAX1* is a high-affinity calcium transporter and plays a role in cytosolic Ca^{2+} concentration control. The cation specificity of *CAX2* is broad (Ca^{2+}, Mn^{2+}, and Cd^{2+}), while *CAX1* is sensitive to cytosolic Ca^{2+}. *CAX3* is very similar to *CAX1* and is involved in cellular ion homeostasis associated with *CAX1* with an inhibition of excess Ca^{2+}. *CAX4* translocates heavy metal ions such as Cd^{2+}, Zn^{2+}, and Mn^{2+}. As *AtCAX2, AtCAX5*, and *AtCAX6* have high homologous identity, it is predicted that they have similar cation selectivity [12, 14, 15]. Other *CAX*s from various plants are presumed to also transport several metal ions; however, detailed information has not been published.

Although there are many pieces of research on ionic homeostasis, no one has ever studied the physical stress-induced effects on *AtCAX5* gene transformant yeast. In this study, we examine what responses ion transport can make under the external ELF-EMF. We chose *AtCAX5* transport because it is associated with both divalent and monovalent cations. To investigate the different types of ELF-EMF effects on the cation sensitivity of *AtCAX5*, we cloned an *AtCAX5* gene from *Arabidopsis thaliana* and expressed it in *Saccharomyces cerevisiae* mutant K667. *S. cerevisiae* K667 is a specific yeast mutant strain in which the vacuolar Ca^{2+} ATPase (PMC1) and H^+/Ca^{2+}antiporter (*VCX1*) were excluded. According to experimental results dealing with various EMF conditions on bacteria [16, 17] and yeast [18–20], it has already been shown that 50-60 Hz, 0.1-0.5 mT AC (alternating current) EMF alters a gene expression and an ion transport [2, 8, 9, 11, 21–24]. In addition, there are a few references that report the cellular effects of different types of current waves. We, therefore, also chose an EMF condition of 60 Hz, 0.1-mT EMF, and evaluated the uptake of Ca^{2+}, K^+, Na^+, Zn^{2+} in *p*YES2 empty vector transformant yeast strains and *p*YES2-*AtCAX5* vector transformant yeast strains under different waveforms, namely sinusoidal and square waves.

2 Materials and methods

2.1 Characteristics of *AtCAX5*

Phylogenetic analysis was done using MEGA 5.10 [25] and compared with a number of references. Transmembrane helices in *AtCAX*s were predicted by the TMHMM algorithm [26]. The position and pattern of the helical structure of the *AtCAX*s were compared to each other, and the function was predicted by consulting the previous research. Homology analysis of the *AtCAX* family was performed using the online program BLAST [27].

2.2 EMF exposure system and experimental design

The ELF-EMFs were generated by a cylindrical solenoid with an internal diameter of 17 cm and length of 28 cm, with 600 turns of copper wire (Fig. 1). This device produced a spatially homogeneous magnetic field with 60-Hz frequency and adjusting intensity at 0.1 mT within the coiled cylinder. The field was generated by a weak current at ~ 4 mA in order to avoid a heat induced from our system. Sample tubes that contained cell samples were fixed with polystyrene foam and placed half way along the coiled cylinder so as to produce a homogeneous magnetic field for all the samples. Polystyrene foam with sample tube holes was used to fix the sample tubes in the center of coil cylinder. Before placing samples, we tested the intensities at each sample hole. The field intensity was confirmed by Gauss meter measurements (LZ-640, Linkjoin Technology, Loudi, Hunan, China). The magnetic field intensity within the coiled solenoid cylinder was stable at 0.1 mT. Therefore, we ensured that all samples located within the solenoid cylinder would receive the same electromagnetic effect. The solenoid was fed from a signal generator (AFG 2021-SC, Tektronix, Shanghai, China), and the AC voltage that was applied was modulated to attain 0.1-mT magnetic field intensity.

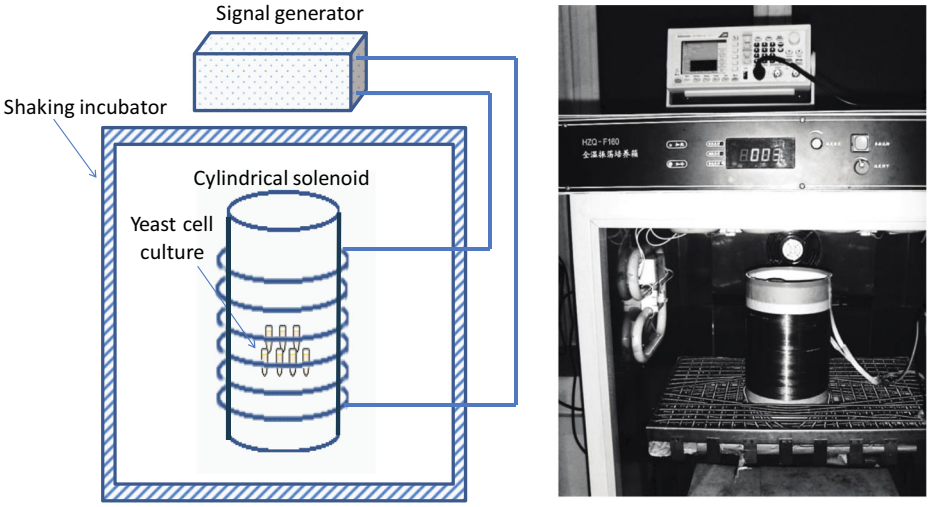

Fig. 1 Diagram of EMF generated incubator for ELF-EMF exposure during the incubations; 1.5-ml microtubes containing yeast culture were placed in 17-cm-diameter and 28-cm-long cylindrical solenoid with 600 turns of copper wire. A signal generator was used to generate sine or square waves of ELF-EMF at 60 Hz. The intensity of the magnetic field was measured as 0.1 mT

The solenoid was placed vertically in the oscillation incubator (HZQ-F1600, Nanjing Ascent Technology Development, Nanjing, China) as shown in Fig. 1. When samples were incubated under different EMF exposures, oscillations of 120 rpm and a temperature of 30 °C were applied. In addition, system oscillation in the incubator was applied to eliminate the temperature change in the solenoid during the incubation under the EMF exposure. Culture samples were exposed to 60-Hz, 0.1-mT sinusoidal or square magnetics waves for 5, 10, 15, and 20 min, respectively. A control was located in the same solenoid and kept for 20 min without applying an EMF. Subsequently, cations were extracted with 0.1 M HCl for 4 h. The experiment was performed in triplicate.

2.3 Microbe strains and vectors

Plasmids were selected and propagated in *Escherichia coli* strain JM109. The Ca^{2+}-sensitive *S. cerevisiae* strain K667 (MATa cnb1::LEU1 pmc1::TRP1 vcx1 Δ ade2-1 can1-100 his3-11, 15 leu2-3112 trp1-1 ura3-1) was used for our yeast assays [28]. The *AtCAX5* gene was propagated in *p*MD18-T vector (Takara Biotech, Dalian, Liaoning, China) and inserts were transferred to the shuttle vector *p*YES2 for its expression in the yeast.

2.4 DNA manipulations

Total RNA extracted from the shoots of *Arabidopsis thaliana* using TRIzol reagent (Cat. #: 15596026; Invitrogen, Carlsbad, CA, USA). The cDNA sequence for the *AtCAX5* (At1g55730) coding region was obtained from the *Arabidopsis* Information Resource (TAIR). *AtCAX5* coding region was amplified by RT-PCR (Gene AMPPCR System 9700, Applied Biosystems, Foster City, CA, USA) using a gene-specific forward primer (5′- GGGATTTC TGCTGCAACTTG -3′) and a reverse primer (5’-GCCCCTAAGGGAAGGTAAAA-3′). The

AtCAX5 PCR product was sub-cloned into a *p*MD18-T vector and completely sequenced using the vector primer (RV-M) in the Beijing Genomic Institute (Beijing, China). The sequencing result was analyzed using BioEdit (Version 7.1.9, Ibis Biosciences, Carlsbad, CA, USA).

For the construction of yeast expression plasmid *p*YES2-*AtCAX5*, the *AtCAX5* cDNA fragment was amplified by PCR from the plasmid *p*MD18-T-*AtCAX5* using a forward primer 5'-AAGCTTTAGCACAAGTCTATGGGTTG-3′ (with an introduced *Hind*III site underlined) and a reverse primer 5′- GGTACCTGTGTTCCTGAGATCTTCAG-3′(with an introduced *Kpn*I site underlined). The PCR product was ligated into a pYES2 vector (Invitrogen) by digestion with *Hind*III and *Kpn*I to construct the plasmid *p*YES2-*AtCAX5*.

2.5 Generation of transgenic K667 strains expressing *AtCAX5* and growth conditions

The plasmids *p*YES2-*AtCAX5* and empty *p*YES2 were introduced into yeast *Saccharomyces cerevisiae* strain K667 by LiAc/ssDNA/PEG method [29]. Transformants were selected on SD plates without uracil [30].

Cation sensitivity was determined by drop tests in solid YP + 2% galactose (yeast extract, peptone, dextrose; trypong 10 g/l, yeast 20 g/l, galactose 20 g/l, and agar 15 g/l) medium containing different salts including $CaCl_2$, NaCl, KCl, $FeCl_2$, $BaCl_2$, $MnCl_2$, $CdCl_2$, and $ZnCl_2$. Yeast transformants of *p*YES2-*AtCAX5* and empty *p*YES2 were cultured in liquid SD-Ura medium (Cat. No. 630314, Clontech, Takara; containing 0.67% Yeast Nitrogen Base, 2% glucose and 0.08% -Ura amino acid drop out mix) at 30 °C to an absorbance $OD_{600} \approx 1$, and diluted with distilled water (1/10, $1/10^2$, $1/10^3$, $1/10^4$, and $1/10^5$). An aliquot of 5 μl was dropped on the plates. All plates were incubated at 30 °C and growth was monitored for 3 to 7 days.

2.6 Measurement of intracellular cation concentrations

K667 cells introduced with pYES2 and pYES2-AtCAX5 vectors were used as the EMF exposure sample. The samples were cultured in liquid YP + 2% galactose medium under the 60-Hz, 0.1-mT EMF in the coil cylinder for 0-20 min at 5-min intervals. The volume of each sample was 1.5 ml put in an Eppendorf tube. The cultured cells were next centrifuged for 5 min at 2000 × *g* and suspended in uptake buffer (2.0% galactose, 10 mM MES, and pH 6.0) containing 50 mM $CaCl_2$, KCl, NaCl, and 10 mM $ZnCl_2$, respectively. After 4 h, the cells were washed twice with distilled water. Ions from the cells were extracted with 0.1 M HCl for 15 min in 95 °C [31]. After 15,000 × *g* centrifugation for 2 min, the contents of cations were determined by an atomic absorption spectrometer (Perkin Elmer AAnalyst 800, PerkinElmer, Waltham, MA, USA). When using the spectrometer, we measured the potassium and sodium concentrations after diluting to $1/10^6$, unlike calcium and zinc, because the common intracellular concentration of potassium and sodium is in the mM range. Additional $CaCl_2$, NaCl, KCl, and $ZnCl_2$ were used to provide the exogenous cation concentrations.

2.7 Statistical analysis

The results are expressed as mean ± standard error of at least three replicates. Statistical analysis was performed using Student's *t* test. Differences were considered statistically significant for $p < 0.05$.

3 Results

3.1 Bioinformatics analysis of *AtCAX5*

According to phylogenetic analysis (Fig. 2), *CAX* belongs to Ca^{2+}/cation antiporter (CaCA) superfamily. *CAX*s are divided into three phylogenetic subgroups; types I, II, and III [15]. Most plant *CAX*s are known as type I. Figure 2 shows that *AtCAX*s were separated into two groups: type 1A grouping *AtCAX1*, *AtCAX3, AtCAX4*, and type 1B grouping *AtCAX2, AtCAX5*, and *AtCAX6*.

Homology analysis demonstrated that *AtCAX5* has 85.0 and 89.0% amino acid sequence identities to *AtCAX2* (NP_566452) and *AtCAX6* (NP_175968), respectively. *AtCAX2, AtCAX5*, and *AtCAX6*, which are homologous to each other, belong to the common subtype of *CAX* type 1B. These homologous sequence structures suggest that these *CAX*s may transport similar substrate specificity such as Mn^{2+}, Cd^{2+}, or Zn^{2+} [32].

Figure 3 shows the distribution of the alpha helical transmembrane conformation of *AtCAX* family. The common position and pattern of helical structures indicated that *CAX* type 1B could have similar physiological functions. Helical transmembrane structures are known to form pores to transport various ions across membranes. Therefore, structural similarity of *AtCAX5* and *AtCAX6* may indicate the similar cation transports such as Cd^{2+} and Zn^{2+}. Consequently, we chose one of them, *AtCAX5*, for cloning into yeast K667 strain to investigate its characteristics in various exogenous cation stresses and ELF-EMF stresses.

3.2 Extraction and clone of *AtCAX5*

Through PCR with designed primers for *AtCAX5* ORF cloning, we isolated *AtCAX5* DNA from *Arabidopsis thaliana* cDNA. Figure 4a shows the electrophoresis result of PCR product with designed primers (forward primer: 5′- GGGATTTCTGCTGCAACTTG -3′, reverse primer: 5′- GCCCCTAAGGGAAGGTAAAA -3′). The length of DNA was 1604 bp. PCR

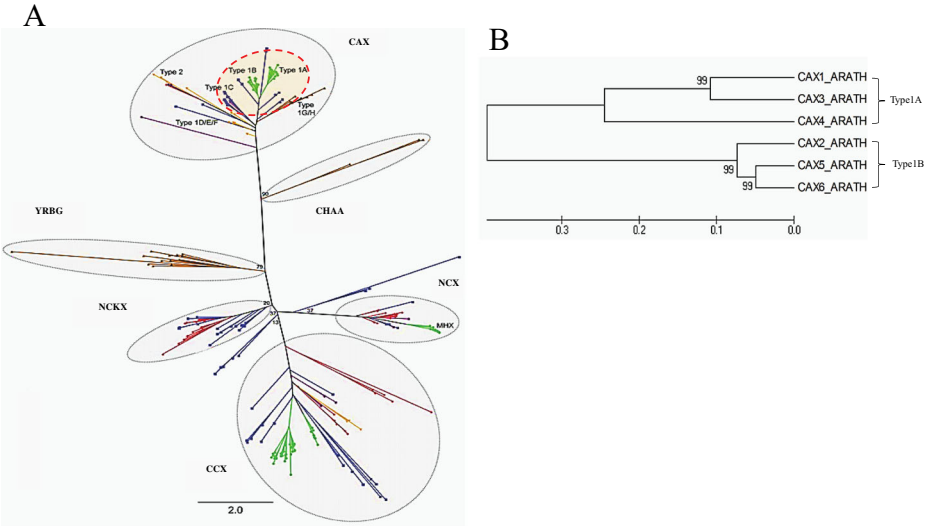

Fig. 2 Phylogenetic analysis of **a** the *CaCA* superfamily (the figure is reprinted from Ref. [15] under a Creative Commons Attribution Non Commercial License, and with the permission of the author) and **b** *AtCAX*s

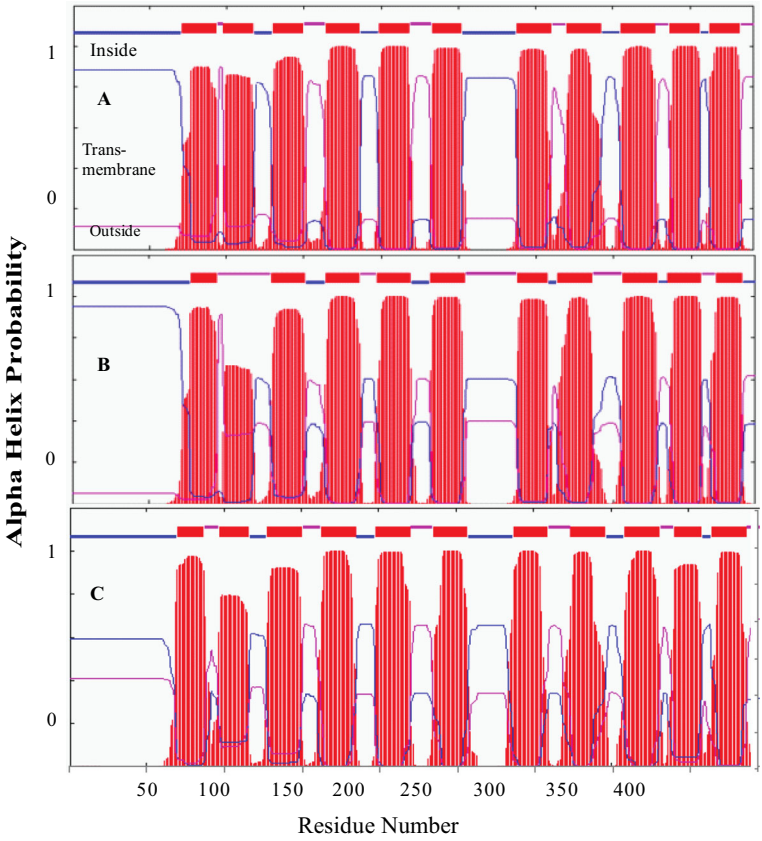

Fig. 3 Topology analysis of type 1B, *AtCAXs: AtCAX2, AtCAX5*, and *AtCAX6*

product was inserted into *p*MD18-T vector, and transformed into *E. coli* JM109. After sequencing, it was confirmed that *AtCAX5* ORF was isolated successfully.

A *p*YES2 vector with a length of 5900 kbp was mainly used for transformation and expression of the target gene into yeast. Figure 4b shows the restricted bands of *p*YES2 and *p*MD18-T-*AtCAX5* vectors by endonucleases *Hind*III and *Kpn*I. *p*YES2 fragment was 5850 bp. *p*MD18-T fragment about 2600 bp, while *AtCAX5* DNA was 1404 bp. Sequencing result of *p*MD18-T-*AtCAX5* plasmids demonstrated that *AtCAX5* ORF consisted of 1326-bp nucleotides encoding 441 amino acids with 48,096-Da molecular weight.

We transformed the *p*YES2-*AtCAX5* vector into the *Saccharomyces cerevisiae* K667 strain by the LiAc/ssDNA/PEG method, and yeast cells were inoculated on SD-Ura plates. We checked the transformation of *AtCAX5* by PCR using Go-Taq polymerase with grown colons as templates. Figure 4c shows that all colons were pYES2-*AtCAX5* transformants.

3.3 Growth of *AtCAX5* transformant yeast under the different cation stresses

In this section, we evaluated the growth responses of *AtCAX5* transformant yeast compared with *p*YES2 under the cationic stresses. We exposed *AtCAX5* transformant K667 strain on YP + 2% galactose plates containing various levels of $CaCl_2$, NaCl, KCl, $FeCl_2$, $ZnCl_2$, $CdCl_2$,

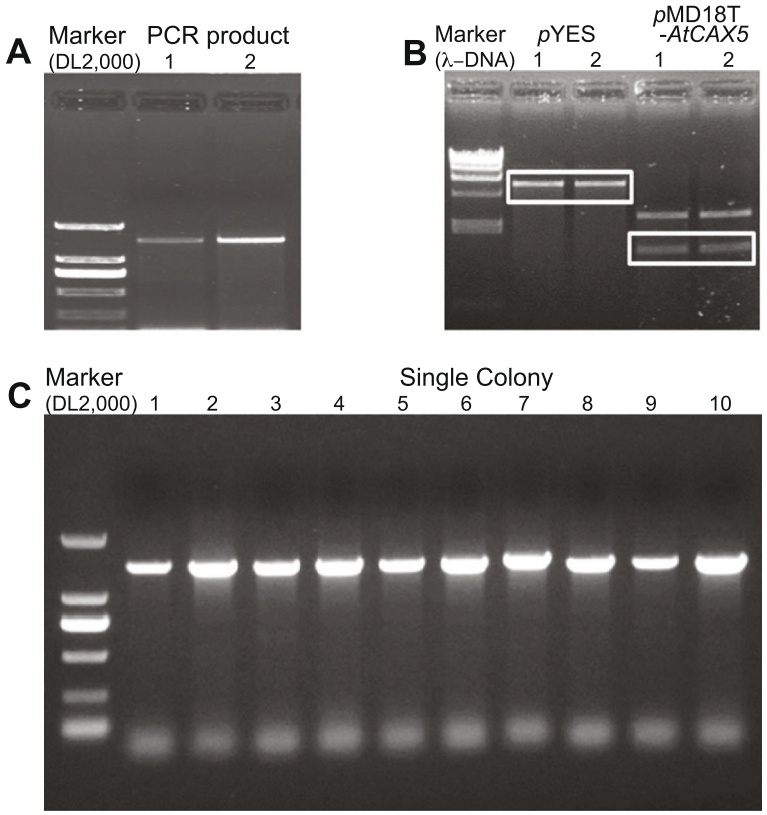

Fig. 4 Gel electrophoresis images of *AtCAX5* cloning PCR; **a** RT-PCR products of *AtCAX5* (product size: 1604 bp) extracted from *Arabidopsis thaliana* cDNA. **b** *p*YES2 vector and *p*MD18-T-*AtCAX5*plamids were digested by *Hind*III and *Kpn*I restriction enzymes. DNA fragments extracted from electrophoresis gel (*marked boxes*). **c** After transformation into yeast K667 strain, colonies transformed *AtCAX5* were checked by PCR using Go-Taq enzyme

$BaCl_2$, and investigated the growth of cells. Empty pYES2 transformant K667 strain was used as a control. As shown in Fig. 5, the growth of *AtCAX5* transformant yeast was hardly inhibited on YP + 2% galactose media containing 100 mM $CaCl_2$, 100 mM KCl, 100 mM NaCl, 20 mM $BaCl_2$, 10 mM $ZnCl_2$, 10 mM $FeCl_2$, and 0.5 mM $CdCl_2$ showing the almost same growth ability on YP + 2% galactose media without metal ions. However, in the control group, it was demonstrated that the same cation concentration inhibited yeast growth significantly.

CAXs have been reported to regulate Ca^{2+} uptake into vacuoles under excessive Ca^{2+} stresses [14]. For further understanding of the cation stress tolerance effect of *AtCAX5*, we investigated the alteration of Ca^{2+} absorption caused by *AtCAX5*. Therefore, *AtCAX5* transgenic yeasts and controls were subjected to 50 mM ~ 250 mM $[Ca^{2+}]_{ext}$ stress to determine the *AtCAX5*-induced Ca^{2+}tolerance. *AtCAX5* transformed yeast showed higher Ca^{2+} uptake ability in general under an exogenous concentration of Ca^{2+}stresses compared with the control (Fig. 6a). In contrast with control lines, as $[Ca^{2+}]_{ext}$ increased from 50 mM to 250 mM without EMF exposure, the Ca^{2+}uptake of expressed *AtCAX5* lines increased 0 ~ 30%. Our measurements of $[Ca^{2+}]_{int}$ included the intra-vacuolar concentration of Ca^{2+}. From the above results, it can be concluded that $[Ca^{2+}]_{int}$ increment in expressed *AtCAX5* lines compared to the control

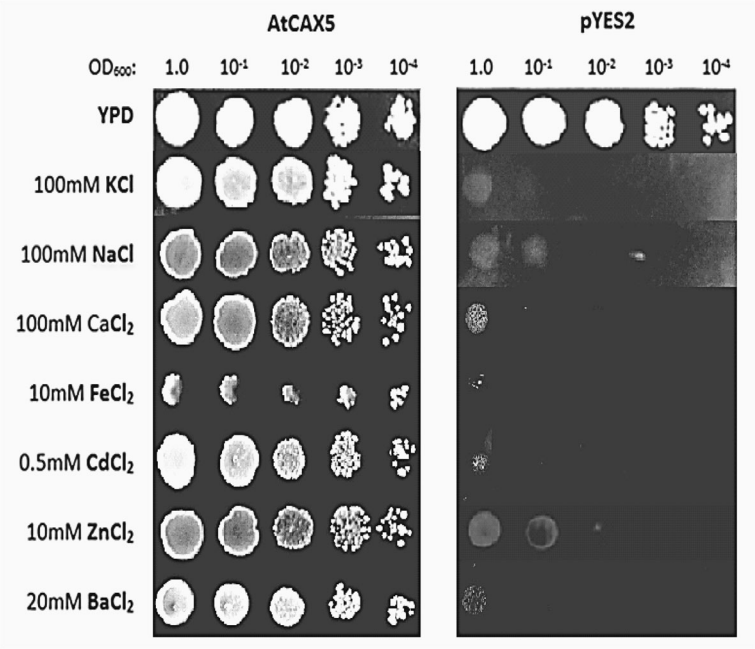

Fig. 5 Growth of yeast (*Saccharomyces cerevisiae* K667) cells transformed with empty vector *p*YES2 (control) or with the *p*YES2 vector containing *AtCAX5* cDNA (*p*YES2-*AtCAX5*). Yeast cells were incubated for 3 days on YP + 2% galactose plates under the indicated concentrations of various cation chlorides with serially dilution of yeast cell suspensions

group was caused by the additional Ca^{2+} accumulation in vacuoles by *AtCAX5* uptakes. The increased-accumulation of Ca^{2+} into vacuoles seems to contribute to the homeostasis of intracellular ions, resulting in the enhanced viability of *AtCAX5* transformant yeast.

3.4 Ion uptake in *AtCAX5* transformant yeast under EMF conditions

The effects of 60-Hz, 0.1-mT sinusoidal EMF on Ca^{2+} uptake were evaluated in the presence of 50 ~ 250 mM $[Ca^{2+}]_{ext}$. Figure 6a shows that for no EMF exposure, the intracellular Ca^{2+}, $[Ca^{2+}]_{int}$, changes according to the exogenous Ca^{2+}, $[Ca^{2+}]_{ext}$. It seemed that $[Ca^{2+}]_{int}$ were in proportion to $[Ca^{2+}]_{ext}$. As $[Ca^{2+}]_{ext}$ increased, $[Ca^{2+}]_{int}$ increased in both *AtCAX5* transformant yeast and the control group; however, $[Ca^{2+}]_{int}$ was always higher in the former than in the control group. This demonstrated that *AtCAX5* accumulated some of the excess intracellular ions into vacuoles to maintain the cytosolic ionic concentration at a homeostatic level. As $[Ca^{2+}]_{ext}$ increased, the enhanced uptake of Ca^{2+} into vacuoles by *AtCAX5* expression resulted in an overall increment of $[Ca^{2+}]_{int}$, which was significantly higher than $[Ca^{2+}]_{int}$ in the control group without *AtCAX5* expression, but there was no significant change for 150 mM and 200 mM $[Ca^{2+}]_{ext}$.

For EMF exposure under the various $[Ca^{2+}]_{ext}$ stress conditions, EMF exposure itself enhanced Ca^{2+} uptake significantly for both control and AtCAX5 expressing yeast strains. EMF-induced $[Ca^{2+}]_{int}$ was found to be 10-60 times higher than those without the EMF exposure (Fig. 6b–e). These results showed that the presence of EMF itself had a significant

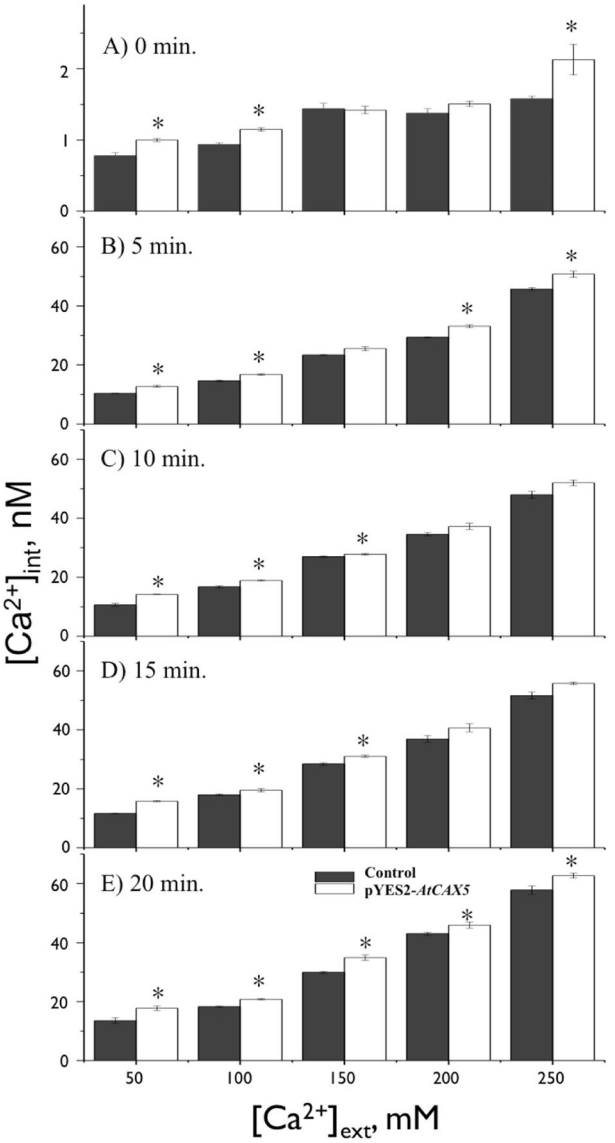

Fig. 6 Measurements of $[Ca^{2+}]_{int}$ under different $[Ca^{2+}]_{ext}$ stress in yeasts transformed with empty *p*YES2 vector or with *p*YES2-*AtCAX5* vector. EMF (60 Hz and 0.1 mT) was applied; **a** for 0 min, **b** for 5 min, **c** for 10 min, **d** for 15 min, and **e** for 20 min. * indicates for $p < 0.05$ verse corresponding control

impact on the function of all transport proteins located in both cytosolic and vacuolar membrane (*AtCAX5*), and resulted in the Ca^{2+} uptake through cellular membranes.

In addition, we tested the effects of the wave types of EMF, sinusoidal, and square wave with the same frequency (60 Hz) and magnetic flux density (0.1 mT). In this test, we applied 50 mM exogenous $CaCl_2$. The exposure of both sinusoidal and squared EMF wave types increased $[Ca^{2+}]_{int}$ significantly for both *AtCAX5* transformed yeast and control strains ($p < 0.05$). The increments of $[Ca^{2+}]_{int}$ depended on exposure time, but the pattern of each

EMF effect was different. The increment slope of the sinusoidal EMF effect was lower than that of the square wave EMF effect, but the quantitative increments of $[Ca^{2+}]_{int}$ were bigger under sinusoidal EMF exposure than that under square wave EMF (Fig. 7a).

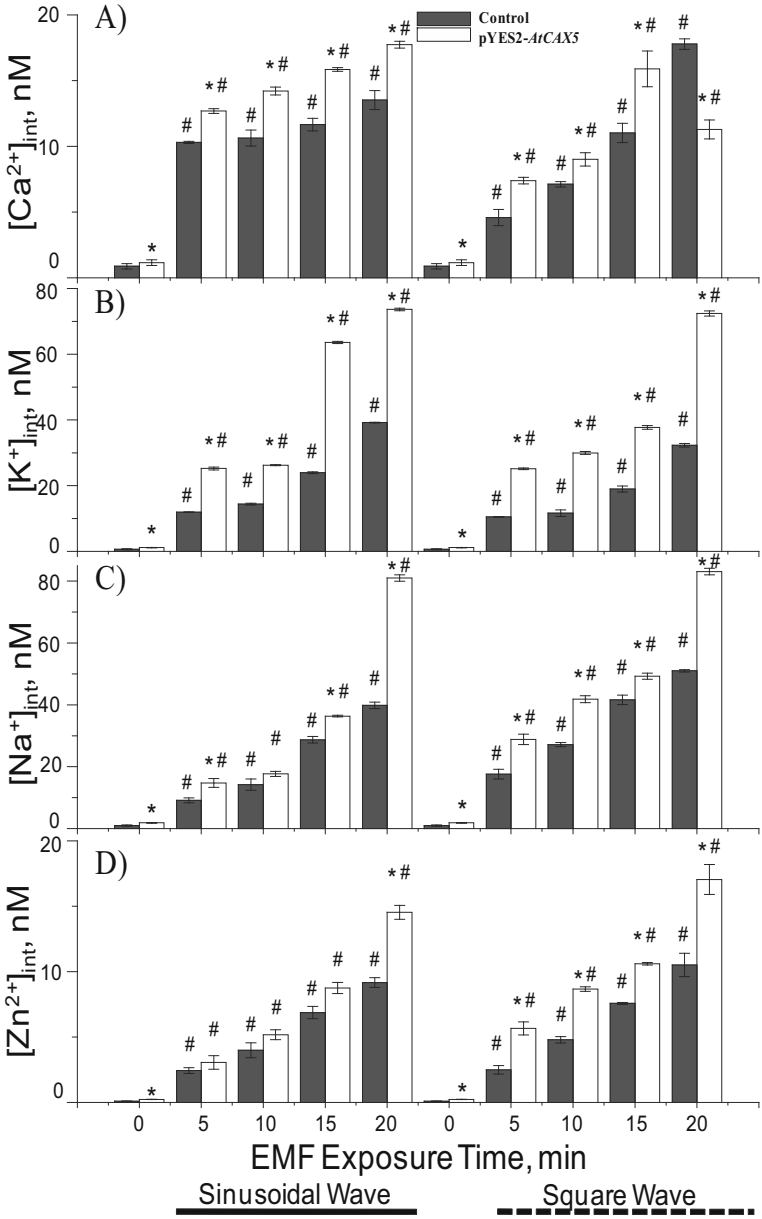

Fig. 7 Measurements of intracellular cations. **a** $[Ca^{2+}]_{int}$, **b** $[K^+]_{int}$, **c** $[Na^+]_{int}$, and **d** $[Zn^{2+}]_{int}$, in terms of 60-Hz and 0.1-mT EMF exposure time (0 exposure time indicates without EMF exposure). Exogenous concentration of each cation was fixed at 50 mM. Each cation measurement was obtained from both sinusoidal (marked ——) and square (marked - - - - - -) waved ELF-EMF exposure. The means ± SE obtained from at least three independent experiments were given. * indicated $p < 0.05$ versus the corresponding control and # indicates for $p < 0.05$ verse corresponding of empty *p*YES2

Levels of $[Na^+]_{int}$, $[K^+]_{int}$, and $[Zn^{2+}]_{int}$ under 50 mM $[Ca^{2+}]_{ext}$ stresses for *AtCAX5* yeasts were also investigated and compared with the control. The results of EMF exposed yeast cell cultures containing 50 mM KCl, NaCl, $ZnCl_2$ were plotted in Fig. 7b–d. As exposure time to EMFs increased, $[K^+]_{int}$, $[Na^+]_{int}$, and $[Zn^{2+}]_{int}$ of both *AtCAX5* transformed yeast and control strains increased significantly ($p < 0.05$). It seemed that the increments were linear to the EMF exposure time, and the slope of the intercellular cation increment was extracted and listed in Table 1. The slope of the sinusoidal EMF effect was less steep than that of the square wave, except in the case of $[K^+]_{int}$. Regarding the EMF effect on K^+ accumulation, the quantitative increment of $[K^+]_{int}$ was greater under the sinusoidal EMF exposure than that under the square wave EMF (Fig. 7b). In general, $[Na^+]_{int}$ and $[Zn^{2+}]_{int}$ also linearly increased as the exposure time of both sinusoidal and square waved EMFs (Fig. 7b–d). To summarize, all data indicated cation uptakes into vacuoles in *AtCAX5* transformed yeast showed significantly higher accumulation level than that in the control strain, causing a significant change in the level of $[Ca^{2+}]_{int}$ between the *AtCAX5* transformed strain and the control strain.

4 Discussion

With the development of communication using an electromagnetic field, organisms on earth have been exposed to increasing magnetic field, which affects organisms' growth in various ways either negatively or positively. In particular, the effect of EMF on cellular ionic transport has recently been focused on by many researchers [33–35]. The altered magnetic field in the earth's environment has changed the uptake and transportation of nutrients [5], as well as a growth and photosynthesis in plants [36]. The aim of this research is to investigate the effect of EMF on intracellular ionic homeostasis and uptake ability by focusing on a specific ion transporter in a transformed cell, which can also help to prevent the abnormality in intracellular ionic concentration from EMF-induced effects in places with altered EMF. Therefore, one common feature among these experiment results obtained under the various EMF-induced conditions was that EMF enhanced the level of intracellular cation accumulation significantly, and the accumulation rate depended on exogenous cation concentrations (stress).

The difference between *AtCAX5* transformed K667 strains and the control indicated that the *AtCAX5* played an important role in maintaining the intracellular ionic homeostasis by uptaking the excess cytosolic ions into vacuoles. In *AtCAX5* transformants, the measured intracellular ion concentrations, which include the vacuolar ion concentrations, were higher than those in the control, but, according to the statistical analysis (Table 1), the slope difference between *AtCAX5* transformant and the control was not significant. However, reflecting the fact that only the *AtCAX5* transformant survived in the higher exogenous cationic concentration, whereas the control strain hardly grew in the same condition, it is confirmed that *AtCAX5* plays a significant role in maintaining the cytosolic ionic homeostasis. The *AtCAX5* located in the vacuolar membrane mediated the intracellular ion homeostasis by the compartmentation of excess ions into vacuoles. Another possible reason could be that the *CAX*s are closely related to the proton electrochemical gradient, which exists across the tonoplast formed by P-type Ca^{2+} ATPase (Olivier et al. 2010). However, the yeast K667 strain we used was deficient in both Ca^{2+}/H^+ exchanger and Ca^{2+} ATPase, illustrating that transformed *AtCAX5* could not be correlated with the proton gradient generated by yeast Ca^{2+} ATPase, but *AtCAX5* function could be supported from other proton gradient generating pumps or channels. This result indicated that vacuolar *AtCAX5* played a role in maintaining the intracellular ion homeostasis by the compartmentation of excess ions into vacuoles.

Table 1 Increasing rate of $[Ca^{2+}]_{int}$, $[Na^{+}]_{int}$, $[K^{+}]_{int}$, and $[Zn^{2+}]_{int}$ in terms of EMF exposure time. Wave type of EMF caused different effects on intracellular cation accumulations. Sin- and Sq- are for sinusoidal wave and squared wave, respectively

Cation	Ca^{2+}		Na^{+}		K^{+}		Zn^{2+}	
Waveform	Sin-	Sq-	Sin-	Sq-	Sin-	Sq-	Sin-	Sq-
Control	1.0692 ± 0.9064	4.2513 ± 0.8866	10.659 ± 0.9705	11.47 ± 0.9924	9.1277 ± 0.9103	7.274 ± 0.8776	0.4516 ± 0.9933	0.5181 ± 0.9971
AtCAX5	1.677 ± 0.9975	4.3484 ± 0.9538	10.818 ± 0.8504	17.014 ± 0.9005	16.564 ± 0.9818	14.949 ± 0.8161	0.5532 ± 0.9903	0.7709 ± 0.9667

Enhancement of EMF-induced $[Ca^{2+}]_{int}$ and $[Zn^{2+}]_{int}$ was less than that of EMF-induced $[Na^{+}]_{int}$ and $[K^{+}]_{int}$. It has been reported that some Ca^{2+}/H^{+} antiporters also took the role of Na^{+}/H^{+} and K^{+}/H^{+} antiporters, conferring tolerance to a high concentration of cations including Ca^{2+}, K^{+} or Na^{+} [37, 38]. Therefore, it is assumed that *AtCAX5* also acted as a Na^{+}/H^{+} and K^{+}/H^{+} antiport like ChaA, a Ca^{2+}/H^{+} antiporter.

According to the results, the slopes of sinusoidal EMF effect on $[Ca^{2+}]_{int}$, $[Na^{+}]_{int}$, and $[Zn^{2+}]_{int}$ were lower than that of square EMF effect, but vice versa for $[K^{+}]_{int}$ (Table 1). The increased amount of intracellular cation accumulations under EMFs could be considered as the result of EMF effects on cellular ion transporters. Besides transformed *AtCAX5*, the yeast cell had its original ion channels or transporters, which could be affected by EMFs. It was reported that EMF was closely related to voltage-gated ion channels, and the alteration of intracellular ion concentration. However, we assumed that EMF sensing structures of ion transporters of cells such as α-helix structure, which would be allied to form the transmembrane structures, could also alter the transformation characteristics of ion transporters [39].

Overall, our results clearly indicated that *AtCAX5* has a wide range of cation sensitivity similar to type I *CAX*s-*AtCAX2* and *AtCAX6*. Under the 60-Hz, 0.1-mT EMF exposure, $[Ca^{2+}]_{int}$, $[K^{+}]_{int}$, $[Na^{+}]_{int}$, and $[Zn^{2+}]_{int}$ were increased depending on the exogenous cation concentrations. The effect patterns of sinusoidal EMF and square wave EMF vary according to the types of the cations. Significant EMF effects on the *AtCAX5* transformant showed that some kind of ion transporters could be related to an EMF that altered the cellular environment, though they are not specific voltage-gated channels or other EMF-specific channels. Our results demonstrated that ELF-EMF (60 Hz, 0.1 mT) could increase the cation absorption activity of transfected yeast cells, which could be utilized in biomass production containing a large proportion of ions for nutrient food or in bioremediation process in metal-polluted environments.

Compliance with ethical standards

Conflict of interest The authors declare no conflicts of interest.

References

1. Lacy-Hulbert, A., Metcalfe, J.C., Hesketh, R.: Biological responses to electromagnetic fields. FASEB J. **12**, 395–420 (1998)
2. Walleczek, J.: Electromagnetic field effects on cells of the immune system: the role of calcium signaling. FASEB J. **6**, 3177–3185 (1992)
3. Safarik, I., Maderova, Z., Pospiskova, K., Baldikova, E., Horska, K., Safarikova, L.: Magnetically responsive yeast cells: methods of preparation and applications. Yeast **32**, 227–237 (2015)
4. Fanelli, C., Coppola, S., Barone, R.: Magnetic fields increase cell survival by inhibiting apoptosis via modulation of Ca2+ influx. FASEB J. **13**, 95–102 (1999)
5. Pazur, A., Rassadine, V.: Transient effect of weak electromagnetic fields on calcium ion concentration in *Arabidopsis thaliana*. PMC Plant Biol. **9**, 47 (2009)
6. Dubyak, G.R.: Ion homeostasis, channels, and transporters: an update on cellular mechanisms. Adv Physiol Edu **28**, 143–154 (2004)
7. Karabakhtsian, R., Broude, N., Shalts, N., Kochlatyi, S., Goodman, R., Henderson, A.S.: Calcium is necessary in the cell response to EM fields. FEBS Lett. **349**, 1–6 (1994)

8. Lindström, E., Lindström, P., Berglund, A., Lundgren, E., Mild, K.H.: Intracellular calcium oscillations in a T-cell line after exposure to extremely-low-frequency magnetic fields with variable frequencies and flux densities. Bioelectromagnetics **16**, 41–47 (1995)
9. Barbier, E., Veyret, B., Dufy, B.: Stimulation of Ca2+ influx in rat pituitary cells under exposure to a 50-Hz magnetic field. Bioelectromagnetics **17**, 303–311 (1996)
10. Grassi, C., D'Ascenzo, M., Torsello, A., Martinotti, G., Wolf, F., Cittadini, A., Battista, G.A.: Effects of 50-Hz electromagnetic fields on voltage-gated Ca2+ channels and their role in modulation of neuroendocrine cell proliferation and death. Cell Calcium **35**, 307–315 (2004)
11. Craviso, G.L., Poss, J., Lanctot, C., Lundback, S.S., Chatterjee, I., Publicover, N.G.: Intracellular calcium activity in isolated bovine adrenal chromaffin cells in the presence and absence of 60-Hz magnetic fields. Bioelectromagnetics **23**, 557–567 (2002)
12. Mäser, P., Thomine, S., Schroeder, J.I., Ward, J.M., Hirschi, K., Sze, H., Talke, I.N., Amtmann, A., Maathuis, F.J.M., Sanders, D., Harper, J.F., Tchieu, J., Gribskov, M., Persans, M.W., Salt, D.E., Kim, S.A., Guerinot, M.L.: Phylogenetic relationships within cation transporter families of *Arabidopsis*. Plant Physiol. **126**, 1646–1667 (2001)
13. Gadsby, D.C.: Ion channels versus ion pumps: the principal difference, in principle. Nat. Rev. Mol. Cell Biol. **10**, 344–352 (2009)
14. Manohar, M., Shigaki, T., Hirschi, K.D.: Plant cation/H^+ exchangers (CAXs): biological functions and genetic manipulations. Plant Biol. **13**, 561–569 (2011)
15. Emery, L., Whelam, S., Hirschi, K.D., Pittman, J.K.: Protein phylogenetic analysis of Ca^{2+}/Cation antiporters and insights into their evolution in plants. Front Plant Sci. **13,** 1–19. https://doi.org/10.3389/fpls.2012.00001
16. Utsunomiya, T., Yamane, Y.-I., Watanabe, M., Sasaki, K.: Stimulation of porphyrin production by application of an external magnetic field to a photosynthetic bacterium, *Rhodobacter sphaeroides*. J. Biosci. Bioeng. **95**, 401–404 (2003)
17. Cellini, L., Grande, R., Campli, E.D., Bartolomeo, S.D., Giulio, M.D., Robuffo, I., Trubiani, O., Mariggio, M.A.: Bacterial response to the exposure of 50-Hz electromagnetic fields. Bioelectromagnetics **29**, 302–311 (2008)
18. Fiedler, U., Grobner, U., Berg, H.: Electrostimulation of yeast proliferation. Bioelectrochem. Bioenerg. **38**, 423–425 (1995)
19. Nakanishi, K., Tokuda, H., Soga, T., Yoshinaga, T., Takeda, M.: Effect of electric current on growth and alcohol production by yeast cells. J. Ferment. Bioeng. **85**, 250–253 (1998)
20. Perez, V., Reyes, A., Justo, O., Alvarez, D.: Bioreactor coupled with electromagnetic field generator: effects of extremely low frequency electromagnetic fields on ethanol production by *Saccharomyces cerevisiae*. Biotechnol. Prog. **23**, 1091–1094 (2007)
21. Marron, M.T., Goodman, E.M., Greenebaum, B., Tipnis, P.: Effects of sinusoidal 60-Hz electric and magnetic fields on ATP and oxygen levels in the slime mold, *Physarumpolycephalum*. Bioelectromagnetics **7**, 307–314 (1986)
22. Lin, K.-W., Yang, C.-J., Lian, H.-Y., Cai, P.: Exposure of ELF-EMF and RF-EMF increase the rate of glucose transport and TCA cycle in budding yeast. Front. Microbiol. **7**, 1378 (2016). https://doi.org/10.3389/fmicb.2016.01378
23. Novak, J., Strašák, L., Fojt, L., Slaninová, I., Vetterl, V.: Effects of low-frequency magnetic fields on the viability of yeast *Saccharomyces cerevisiae*. Bioelectrochemistry **70**, 115–121 (2007)
24. Wolff, S.A., Coelho, L.H., Karoliussen, I., Jost, A.-I.K.: Effects of the extraterrestrial environment on plants: recommendations for future space experiments for the MELiSSA higher plant compartment. Life **4**, 189–204 (2014)
25. Tamura, K., Peterson, D., Peterson, N., Stecher, G., Nei, M., Kumar, S.: MEGA5: molecular evolutionary genetics analysis using maximum likelihood, evolutionary distance, and maximum parsimony methods. Mol. Biol. Evol. **28**, 2731–2739 (2011)
26. Krogh, A., Larsson, B.: von-Heijne, G., Sonnhammer, E.L.: predicting transmembrane protein topology with a hidden Markov model: application to complete genomes. J. Mol. Biol. **305**, 567–580 (2001)
27. Altschul, S., Gish, W., Miller, W., Myers, E., Lipman, D.: Basic local alignment search tool. J. Mol. Biol. **215**(3), 403–410 (1990)
28. Cunningham, K.W., Fink, G.R.: Calcineurin inhibits VCX1-dependent H^+/Ca^{2+} exchange and induces Ca2+ATPases in *Saccharomyces cerevisiae*. Mol. Cell. Biol. **16**, 2226–2237 (1996)
29. Gietz, R.D., Schiestl, R.H., Willems, A.R., Woods, R.A.: Studies on the transformation of intact yeast cells by the LiAc/SS-DNA/PEG procedure. Yeast **11**, 355–360 (1995)
30. Kawai, S., Phan, T.A., Kono, E., Harada, K., Okai, C., Fukusaki, E.: Transcriptional and metabolic response in yeast *Saccharomyces cerevisiae* cells during polyethylene glycol-dependent transformation. J. Basic Microbiol. **49**, 73–81 (2009)

31. Mulet, J.M., Leube, M.P., Kron, S.J., Rios, G., Fink, G.R., Serrano, R.: A novel mechanism of ion homeostasis and salt tolerance in yeast: the Hal4 and Hal5 protein kinases modulate the Trk1-Trk2 potassium transporter. Mol. Cell. Biol. **19**, 3328–3337 (1999)
32. Pittsman, J.K.: Vacuolar Ca^{2+} uptake. Cell Calcium **50**, 139–146 (2011)
33. Nevzgodina, L.V.: Fundamentals for the assessment of risks from environmental radiation. In: Chromosomal Aberrations as a Biomarker for Cosmic Radiation (NATO Science Series), pp. 203–208. Springer, Houten (1999)
34. Ahmad, M., Galland, P., Ritz, T., Wiltschko, R., Wiltschko, W.: Magnetic intensity affects cryptochrome-dependent responses in *Arabidopsis thaliana*. Planta **225**, 615–624 (2007)
35. Wolff, S.A., Coelho, L.H., Zabrodina, M., Brinckmann, E., Kittang, A.I.: Plant mineral nutrition, gas exchange and photosynthesis in space: a review. Adv. Space Res. **51**, 465–475 (2013)
36. Hakala-Yatkin, M., Sarvikas, P., Paturi, P., Mantysaari, M., Mattila, H., Tyystjarvi, T., Nedbal, L., Tyystjarvi, E.: Magnetic field protects plants against high light by slowing down production of singlet oxygen. Physiol. Plant. **142**, 26–34 (2011)
37. Ivey, D.M., Guffanti, A.A., Zemsky, J., Pinner, E., Karpel, R., Padan, E., Schuldiner, S., Krulwich, T.W.: Cloning and characterization of a putative Ca^{2+}/H^+ antiporter gene from *Escherichia coli* upon functional complementation of Na^+/H^+ antiporter-deficient strains by the overexpressed gene. J. Biol. Chem. **268**, 11296–11303 (1993)
38. Olivier, C., Maria, N.A., Marina, L., Maria, P.R., Kees, V.: Vacuolar cation/H^+antiporters of *Saccharomyces cerevisiae*. J. Biol. Chem. **285**, 33914–33922 (2010)
39. Panagopoulos, D.J., Karabarbounis, A., Margaritisa, L.H.: Mechanism for action of electromagnetic fields on cells. BBRC **298**, 95–102 (2002)